Multitechnique surface analysis of poly(*N*-vinylpyridine-*co*-styrene) and poly(*N*-vinylimidazole-*co*-styrene) random copolymers

Helen F. Lee* and Joseph A. Gardella Jr†
Department of Chemistry, State University of New York at Buffalo, Buffalo, NY 14214, USA
(Received 26 September 1990; revised 30 September 1991; accepted 11 October 1991)

The surface structure and bulk compositions of random copolymer systems based on poly(*N*-vinylpyridine) ($N = 2, 4$) and poly(*N*-vinylimidazole) copolymerized with polystyrene were examined by X-ray photoelectron spectroscopy (X.p.s.) or electron spectroscopy for chemical analysis, Fourier transform infra-red spectroscopy (*FT*i.r.) and static secondary ion mass spectrometry (s.i.m.s.). The spectroscopic results were correlated with morphology determined from scanning electron microscopy (SEM) and transmission electron microscopy (TEM). The X.p.s. results from solution-cast thick films and films cast at the air/water interface from poly(*N*-vinylpyridine-*co*-styrene) copolymers indicate equivalent surface and bulk compositions for all angle- and energy-dependent measurements, which are further supported by *FT*i.r. and EM analyses. On the other hand, surface enrichment of polystyrene was observed in angle-dependent X.p.s. analysis of poly(*N*-vinylimidazole-*co*-styrene) preparations. Attenuated total reflectance and transmission i.r. peak intensity ratios are equivalent, which suggests that segregation of polystyrene in the poly(*N*-vinylimidazole-*co*-styrene) system is localized to a region less than 30 Å from the air/polymer interface. In addition, the s.i.m.s. technique was shown to be sensitive to structural differences arising from pH changes as well as to the detection of dimer ions in these systems.

(Keywords: surface structure; composition; random copolymers)

INTRODUCTION

The utility of random copolymers offers advantages of versatility, synthetic ease and lower cost in many areas of polymer science and technology, in comparison to other copolymer systems. The commercial applications of random copolymers range from amorphous elastomers to synthetic rubber and fibre materials in the automotive, packaging and building construction industries[1,2]. Since much of a polymer's performance and end use ultimately depends on its chemical and physical behaviour at interfacial regions, the industrial applications of polymer surface characterization have become an increasingly demanding area of research and development. Consequently, the understanding of polymer surface properties is of great concern because of the vital role played by the outermost atomic layers of these materials in various technological devices and processes.

Microphase heterogeneities are commonly observed phenomena in block copolymer systems, generally attributed to dissimilarities in the chemical and physical composition of the constituent homopolymer blocks[3]. Random copolymer systems on the other hand, are generally single phase, homogeneous systems[4]. Theoretically, random copolymers exhibit average properties of statistically weighted hybrids of the comonomer units[5]. The degree of randomness in a given random copolymer system depends on the relative composition and reactivities of the repeat units. The main objective in this study is to investigate the extent of homogeneity in a series of nitrogen-containing random copolymers. A second goal is to determine whether different sample preparations under selective conditions can induce microphase speciation at the near-surface region in a specific random copolymer system.

Previously, researchers in our laboratory have employed ion and electron spectroscopic techniques to examine the surface characteristics of various polymeric materials[6–11]. Multitechnique surface analyses of these systems have probed into the roles of surface energetics, crystallinity, structure, functional group distribution, orientation and morphology in multicomponent polymers. In the present study, a combination of analytical spectroscopic and microscopic techniques are utilized to evaluate the surface characteristics of a series of nitrogen-containing random copolymers. The experimental emphases are directed at a deeper understanding of the possible control of surface microstructural and morphological behaviours through selection of experimental determinants.

In particular, on these systems, the pyridyl moieties of poly(vinylpyridine)s are chemically reactive sites, attributable to the nucleophilic and weakly basic nature of the aromatic nitrogens. Chemical modifications in vinylpyridine-containing species have led to a wide variety of industrial applications, including catalysis, metal chelations and ion exchanges. A particularly

*Current address: US Patent and Trademark Office, Crystal Mall Bldg, 5th Floor B-19, Crystal City, VA 22202, USA
†Author to whom correspondence should be addressed

0032-3861/92/204250-10

interesting preparation is the charge mosaic membrane derived by quaternization of poly(vinylpyridine) moieties and sulphonation of polystyrene segments in the block copolymers. These membrane materials were shown to exhibit water permeability and salt rejection capacities in piezodialysis experiments[12–14].

Hook and co-workers have studied homopolymers of poly(*N*-vinylpyridine) ($N = 2, 4$) and their derivatives using low energy ion scattering spectroscopy and static secondary ion mass spectrometry (s.i.m.s.) to explore the orientational and structural features at their topmost surface regions[8,10].

The practical applications of *N*-vinylimidazole polymers are also numerous, ranging from dyestuffs, catalysts, corrosion inhibitors, ion exchange resins to their utility in quenching media and metal ion complexations[15,16]. Earlier conformational studies of poly(*N*-vinylimidazole)–polystyrene random copolymers in dilute solutions and cast films have shown evidence of phase separation of imidazole and styrene domains in aqueous media[15]. According to the reported fluorescence and turbidimetric titration results, a conformational change of these copolymers from a coil-like structure to an extended chain configuration was observed upon protonation of the imidazole segments. A sharp transition occurs at around pH 4.0. This has been attributed to the aggregation of styrene domains through attractive hydrophobic interactions and the coulombic repulsions of the charged imidazole segments induced by pH decrease. This in turn has stimulated our interest in studying the surface characteristics of thin film preparations of these random copolymer systems. Specifically, we are interested to see if such microphase separation is observable, and to provide a quantitative evaluation in these random copolymers.

EXPERIMENTAL

Materials and preparations

The random copolymers analysed in this study are listed in *Table 1*. Poly(*N*-vinylpyridine-*co*-styrene) ($N = 2, 4$) random copolymers were purchased from Scientific Polymer Products (Ontario, NY, USA). Poly(*N*-vinylimidazole-*co*-styrene) was obtained from Eastman Kodak Company (Rochester, NY, USA). Two types of sample preparations were used in this study. Solution-cast films were analysed as thick films on cleaned silver (Alfa, 99.999%) coupons cast from 2% (w/w) solutions under nitrogen atmosphere at room temperature. Chloroform (Fisher, certified ACS) and methoxyethanol (Aldrich, anhydrous, 99%) solutions of the copolymers were used. Water-cast films were obtained by placing drops of 2% (w/w) copolymer solution on triply deionized water adjusted to the desired pH. Subsequently, thin films were lifted off the water surface directly onto 200-mesh (3 × 3 mm) copper grids (Ladd Research Industries) and dried under a stream of nitrogen. Prior to spectroscopic analysis, solution-cast films were cleaned by ultrasonic extraction in hexanes to remove surface silicone impurities to below X-ray photoelectron spectroscopy (X.p.s.) detection limits. Water-cast films were analysed without further treatments. No silicone impurities were detected in these preparations.

Instrumentation

X-ray photoelectron spectroscopy. Energy- and angle-dependent X.p.s. characterization of solution-cast thick films were performed on a Perkin-Elmer Physical Electronics PHI-5300 instrument equipped with a 180° hemispherical energy analyser and a multichannel detector. MgKα (1253.6 eV) and TiKα (4510.9 eV) radiation were used as excitation sources, operated at 300 W, 15 kV and 20 mA. A base pressure less than 2.67×10^{-7} Pa and an operating pressure of less than 1.33×10^{-6} Pa were maintained during analysis periods. The energy resolution was established with sputtered silver to produce a Ag $3d_{5/2}$ peak with a binding energy of 367.9 eV and a full width at half maximum (*FWHM*) of 1.00 eV at 800 000 counts per second. The linearity of the energy scale was calibrated using Cu $2p_{3/2}$ and Cu $3p_{3/2}$ lines at 932.5 eV and 75.0 eV, respectively. Under these operating conditions data were collected at resolutions of 0.1 eV per step with MgKα and 0.2 eV per step with TiKα anodes, and pass energies of 35.75 eV

Table 1 Structures and compositions of nitrogen-containing random copolymers

Sample	Structure	Composition (wt%)	Abbreviation
Poly(*N*-vinylimidazole-*co*-styrene)	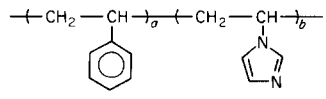	70/30[a]	PVIS
Poly(2-vinylpyridine-*co*-styrene)	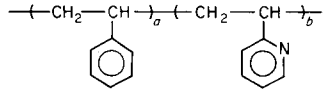	70/30	P2VPS
Poly(4-vinylpyridine-*co*-styrene)	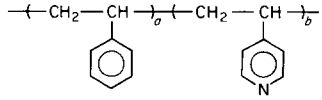	50/50	HP4VPS
Poly(4-vinylpyridine-*co*-styrene)	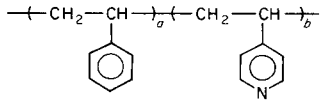	90/10	P4VPS

[a]Molar ratio

and 71.55 eV, respectively. Take-off angles of 10°, 45° and 90° were utilized for the angle-dependent measurements with the MgKα source, corresponding to sampling depths of 18 Å, 73 Å and 103 Å, respectively[17]. Data manipulation (background subtraction, peak integration and curve fitting) was processed on a Perkin-Elmer 7500 computer with PHI ESCA version 2.0 software.

Water-cast films were analysed with a monochromatized AlKα (1486.7 eV) X-ray source on a Surface Science Instruments model SSX-206 spectrometer, operated at 50 W, 10 kV and 5 mA. This instrument also utilized a hemispherical analyser. A base pressure of 1.33×10^{-7} Pa and an operating pressure of 2.0×10^{-6} Pa were maintained during data acquisition periods. The energy scale was calibrated using the Cu $2p_{3/2}$ and Au $4f_{7/2}$ peaks at 932.5 eV and 84.0 eV, respectively. High resolution spectra were recorded with a pass energy of 50 eV and a spot size of 300 μm at 35° analysis angle. A practical resolution of 0.05 eV per channel, 128 channels was defined by using sputtered gold to give a Au $4f_{7/2}$ peak at 84.0 eV with a *FWHM* of 0.88 eV at 170 500 counts-eV s^{-1}. Data processing was carried out with a Hewlett-Packard 9836C computer with SSI ESCA version 8.01A software.

X.p.s. results reported here are averages of 6–12 samples prepared under identical experimental conditions. Typically, angle-dependent measurements were accomplished in 18 min, during which no X-ray damage to the polymers was observed. All peaks were charge corrected by setting the aliphatic (CH_x) peak in the carbon 1s core level region to a binding energy of 285.0 eV.

Fourier transform infra-red spectroscopy. Transmission (t.X.m.) and attenuated total reflectance (a.t.r.) spectra were acquired using a Nicolet 7199A Fourier transform infra-red spectrometer with a liquid nitrogen cooled mercury/cadmium/telluride detector operated at 4 cm^{-1} resolution. A.t.r. spectra were collected with a Harrick XBC-50N beam condenser with internal reflection elements of 45°, 60° KRS-5 and 60° Ge crystals. T.X.m. spectra were collected by casting copolymer solution directly onto NaCl plates. A total of 10 000 scans for a.t.r. and 1000 scans for t.X.m. were averaged and subsequently ratioed to a.t.r. and t.X.m. background to obtain the absorbance spectra.

Static secondary ion mass spectrometry. S.i.m.s. analysis was performed on a quadrupole-based Leybold-Heraeus model LHS10 SIMS spectrometer as described in detail previously[18]. A continuous 4 keV Ar^+ beam was used as the primary ion source. Samples (17 × 8 mm) were mounted on an isolated bias rod. The system is differentially pumped to a base pressure of 2.0×10^{-8} Pa with an operating pressure of 2.0×10^{-6} Pa. During spectral acquisition, the ion beam was defocused and rastered over a 4 × 4 mm analysis area on the polymer surface. A +13.0 V d.c. bias was applied to the bias rod to enhance secondary ion extractions into the mass spectrometer. In all cases, the sample current density was kept below 1 nA cm^{-2} (ion dosage = 1×10^{13} ions cm^{-2}) as measured with a Faraday cup. An auxiliary flood gun operated at electron energy of 50–100 eV was employed to neutralize excess charge build-up during the analyses of thick films.

Positive s.i.m.s. spectra were acquired using an IBM PC-based interface system designed to control quadrupole functions and data processing[18]. Typically, four data points per mass unit corresponding to a resolution of 0.25 amu were collected at a rate of 10 msec per mass unit. Specific mass windows of interest were set up for a particular sample under identical resolutions.

Electron microscopy. SEM micrographs were collected with a Hitachi model S-570 scanning electron microscope equipped with a LaB_6 gun. Samples were mounted on aluminium stubs with silver glue to maintain a conductive pathway to the metal stage. In order to minimize excess charging, samples were rendered conductive by sputter-coating them with chromium in a vacuum evaporator. Typically, an accelerating voltage of 2–4 kV was employed and SEM micrographs were taken at 30° sample tilt angle. TEM analyses were carried out with a Hitachi model HS-8 transmission electron microscope operated at 50 kV. Water-cast thin films were prepared on 200-mesh copper grids as described earlier. They were then coated with carbon in a vacuum evaporator. Direct morphological observations proceeded without staining, since sufficient contrast was achievable in these films. Bulk morphology of poly(*N*-vinylimidazole-*co*-styrene) thin films was observed to be comparable to those observed in an earlier study[15].

Contact angle measurements. Advancing contact angles were measured in air at 25°C by the sessile drop method, using a Rame Hart model 100 goniometer attached to a X–Y travelling microscope, fixed to an optical bench. Drops of triply deionized water at pH values of 1–13 were deposited on the solid surface of solution-cast films with a flame-cleaned Pt wire. The angle of water droplets at each pH value was measured five times.

^{13}C n.m.r. spectroscopy. ^{13}C n.m.r. analyses of polystyrene, poly(2-vinylpyridine), poly(4-vinylpyridine) and their respective copolymers were performed on a Varian Gemini-300 spectrometer operated at 75.5 MHz. ^{13}C spectra of polymer solution (50 mg ml^{-1}) in $CDCl_3$ were acquired at room temperature in the proton-decoupled mode without NOE. A total of 2000 scans were collected for each sample.

RESULTS

X-ray photoelectron spectroscopy

Two types of compositional information are available from X.p.s. analysis. Elemental compositions can be derived from atomic ratios of integrated peak areas, generally charged corrected to the core level carbon 1s peak. Secondly, curve resolution analysis of appropriate core level elemental regions (i.e. C 1s, N 1s) can be analysed to yield concentrations of particular functional groups at the surface[7]. Both types of chemical information can be obtained as a function of sampling depth via variations in X-ray sources (i.e. energy-dependent X.p.s.)[19] and/or proper manipulation of sample stage geometry (i.e. angle-dependent X.p.s.)[7].

In the present study, X.p.s. data were processed with both quantitative approaches. First, experimentally derived N/C peak area ratios are corrected by applying empirically determined sensitivity factors, which were derived from pure homopolymers and model polymeric compounds[20,21]. This quantitation approach takes into account the photoemission cross sections, instrumental

Table 2 Corrected angle-dependent X.p.s. N/C peak area ratios of solution-cast films

Sample	10° (18 Å)	45° (73 Å)	90° (103 Å)	90° (215 Å)	Bulk ratios
PVIS	0.15	0.23	0.24	0.24	0.24
P2VPS	0.09	0.10	0.10	0.10	0.10
HP4VPS	0.06	0.06	0.07	0.07	0.07
P4VPS	0.09	0.10	0.10	0.10	0.13

Table 3 Comparison of N/C ratios between solution-cast and water-cast films

		Water-cast films		
Sample	Solution-cast films	pH 3.0	pH 5.7	pH 9.0
PVIS	0.24	0.17	0.16	0.16
P2VPS	0.10	0.10	0.10	0.10
HP4VPS	0.08	0.06	0.06	0.06
P4VPS	0.11	0.11	0.10	0.11

transmission functions and sample morphologies. *Table 2* lists the corrected energy/angle-dependent N/C atomic ratios in solution-cast films and *Table 3* shows their comparison to water-cast films at various pH values. The effective sampling depths of 18, 73 and 103 Å correspond to emission angles of 10°, 45° and 90° with respect to surface plane, based on previous empirical calculations[17]. All poly(*N*-vinylpyridine-*co*-styrene) copolymers yield surface N/C ratios equivalent to the average bulk composition within error limits of ±5% RSD. On the other hand, X.p.s. studies of solution-cast poly(*N*-vinylimidazole-*co*-styrene) films yield a smaller than bulk N/C ratio of 10° take-off angle. This suggests the segregation of polystyrene microdomains at the near-surface region of less than about 30 Å. The corrected N/C ratios derived from emission angles of 45° and 90° (73–215 Å) are equivalent, within error limits. to those calculated for bulk compositions.

The effect of polystyrene surface excess is illustrated in *Figure 1*, which shows the angle-dependent C 1s and N 1s core level regions of poly(*N*-vinylimidazole-*co*-styrene). It is apparent that a lower N/C ratio exists at the 10° take-off angle as compared to those at 45° and 90°. In addition, comparison between solution-cast and water-cast preparations in small spot X.p.s. analysis yielded a smaller N/C ratio in the water-cast films (*Table 3*). These results suggest a higher affinity of the imidazole segments for aqueous media. The X.p.s. technique, however, was not sensitive enough to discern the compositional differences in the water-cast films prepared at different pH values (3.0, 5.7 and 9.0).

Curve resolution analyses of the C 1s and N 1s envelopes were also carried out to determine if functionality differences can be detected as a function of sampling depths and preparations. *Table 4* lists the various functionalities and their corresponding binding energies in the C 1s and N 1s core level regions. In the poly(*N*-vinylimidazole-*co*-styrene) copolymer, a lower percentage C=N (286.5 eV) in the C 1s envelope was observed at 10° analysis angle. This curve fit result coincides with the corresponding lower N/C peak area ratios obtained at this sampling depth. *Figures 2* and *3* show the representative curve fits of C 1s and N 1s regions in the solution-cast and water-cast films at different pH

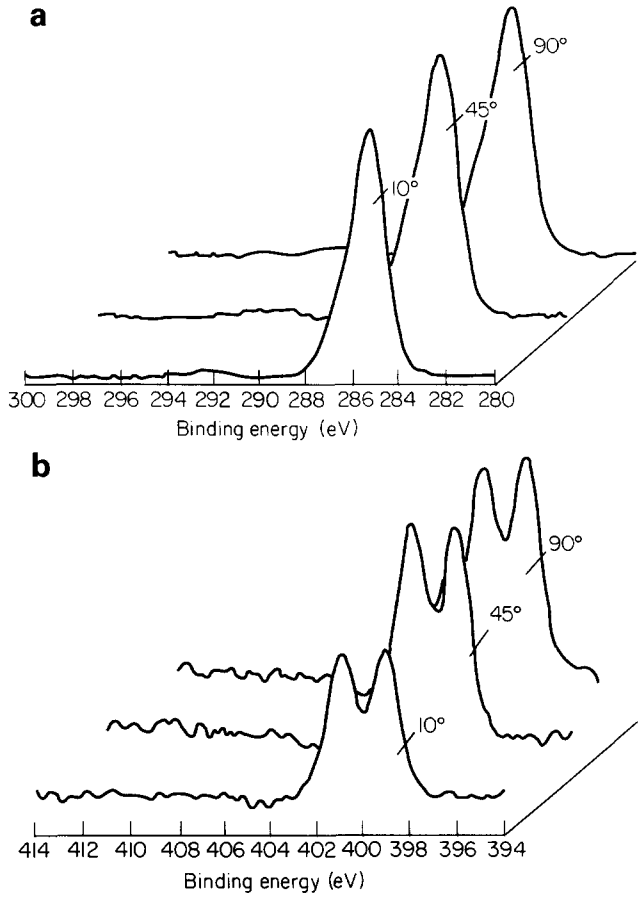

Figure 1 Angle-dependent X.p.s. surface characterization of poly(*N*-vinylimidazole-*co*-styrene): (a) carbon 1s region; (b) nitrogen 1s region

Table 4 High resolution X.p.s. core level peak positions[a]

Core level	Functionality	Binding energy (eV)
C 1s	CH_x	285.0
	C=N	286.5
	$\pi \rightarrow \pi^*$	292.1
N 1s	N=C	398.7
	N–C	400.5
	$\pi \rightarrow \pi^*$	407.0

[a]Models calibrated by comparison to model compounds[24]

values. A smaller C=N percentage was found in the water-cast films (*Figure 2b–d*) which agrees with the corresponding lower N/C integrated peak area ratios in the water-cast preparations. *Table 5* summarizes the curve fit results in these copolymers.

Fourier transform infra-red spectroscopy

A previously developed Beer's law absorbance model[22] was utilized for the calibration of *FT*i.r. results.

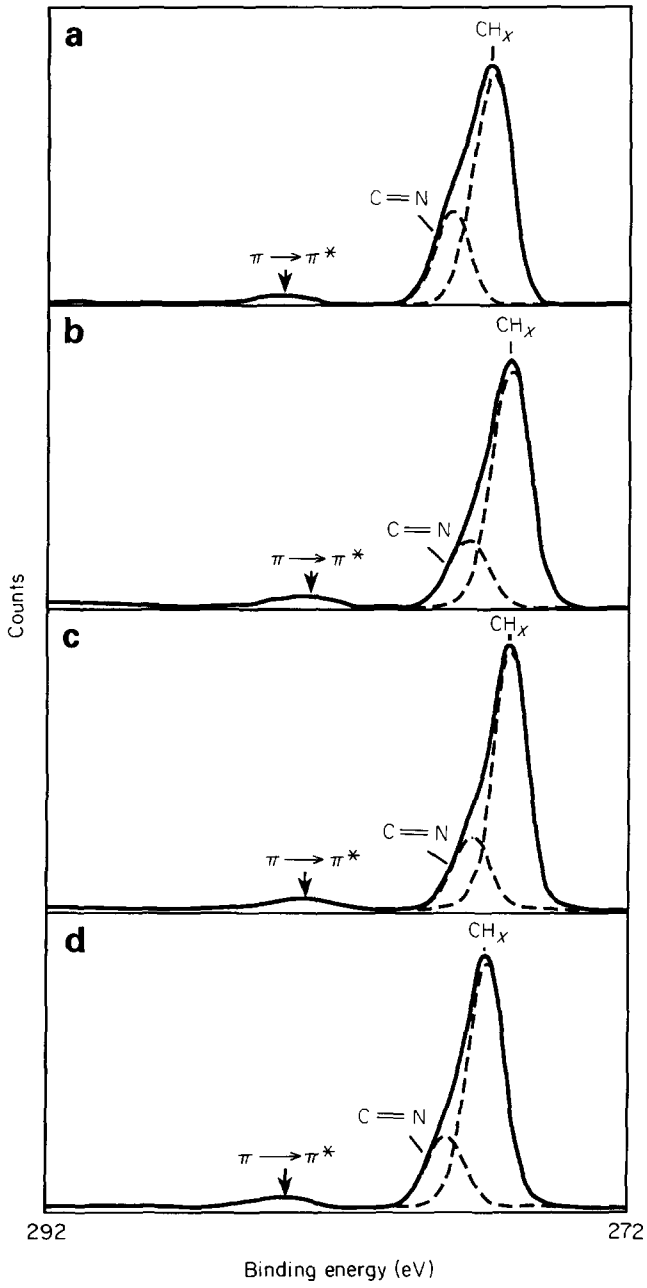

Figure 2 Representative curve fits of carbon 1s core level X.p.s. spectra of poly(*N*-vinylimidazole-*co*-styrene): (a) solution-cast film; (b) water-cast film at pH 3.0; (c) water-cast film at pH 5.7; (d) water-cast film at pH 9.0

In this quantitation approach, transmission bulk analyses of homopolymer blends of known weight, composition, film thickness and pathlength were employed in the determination of molar absorptivities of pure homopolymer materials. The results were then compared to those in a.t.r. and transmission analyses in the corresponding copolymers. *Figures 4a* and *b* show the linear responses in these calibration curves in the poly(*N*-vinylpyridine-*co*-styrene) systems ($N = 2, 4$). *Table 6* summarizes and compares the a.t.r. and transmission peak intensity ratios of the various copolymers in the mid-i.r. regions. In particular, a.t.r. and t.X.m. samplings of poly(*N*-vinylpyridine-*co*-styrene) copolymers yielded similar peak intensity ratios, which confirms the homogeneities in these systems at the micrometre sampling depth and in the bulk. A.t.r. spectra were complicated by a certain amount of band shifts and high absorption background. *Figure 5* shows the ring breathing mode region (1700–1400 cm^{-1}) in these copolymers. Similarly, both a.t.r. and t.X.m. analyses of poly(*N*-vinylimidazole-*co*-styrene) yield equivalent peak intensity ratios within experimental error limits.

Static secondary ion mass spectroscopy

In an earlier static s.i.m.s. study on a series of vinylpyridines and substituted polystyrene homopolymers[8], the distribution of charged stabilized ions (*n*-mer ions) was observed to be directly related to the polymer chain orientation and bonding in their near-surface/interfacial regions. The detailed ion formation mechanism and their subsequent detection have been proposed with inference to the utility of the s.i.m.s. technique in probing

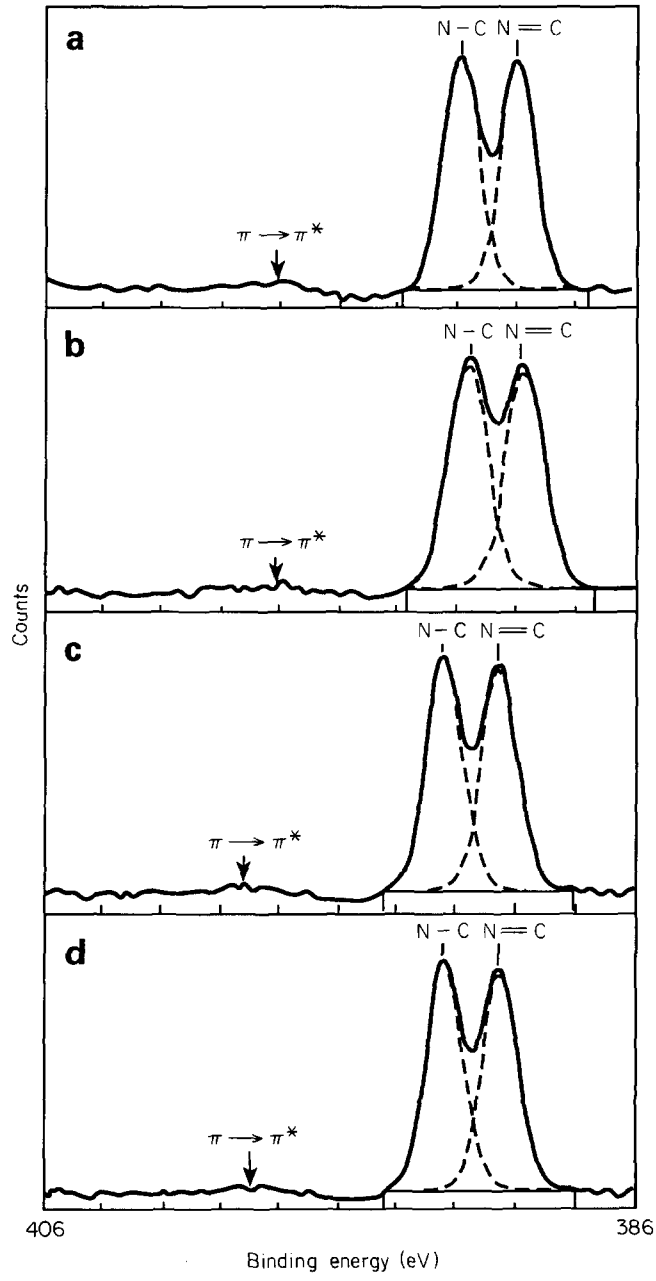

Figure 3 Representative curve fits of nitrogen 1s core level X.p.s. spectra of poly(*N*-vinylimidazole-*co*-styrene): (a) solution-cast film; (b) water-cast film at pH 3.0; (c) water-cast film at pH 5.7; (d) water-cast film at pH 9.0

Table 5 Angle-dependent X.p.s. elemental core level curve fit results

Sample	Analysis angle (deg)	Functionality (%, ±3.5% RSD)					
		CH_x	C=N	$C\pi \rightarrow \pi^*$	N=C	N–C	$N\pi \rightarrow \pi^*$
PVIS	10	86.1	9.6	4.3	48.7	48.5	2.8
	45	75.3	21.0	3.7	49.3	48.5	2.7
	90	76.2	20.3	3.5	49.0	48.6	2.4
P2VPS	10	79.5	15.6	4.9	93.3	–	6.8
	45	80.7	14.3	5.0	92.4	–	7.6
	90	79.8	14.9	5.3	92.8	–	7.2
HP4VPS	10	80.0	14.9	5.1	93.5	–	6.6
	45	82.2	12.4	5.4	92.6	–	7.4
	90	82.5	12.3	5.2	93.2	–	6.4
P4VPS	10	86.8	8.5	4.7	92.7	–	7.3
	45	83.9	11.0	5.1	93.4	–	6.6
	90	84.3	11.1	4.6	92.1	–	7.9

Table 6 Attenuated total reflectance (a.t.r.) and transmission (t.X.m.) *FT*i.r. peak intensity ratios

Sampling	(*N*-Vinylimidazole)/(styrene) comonomers		(2-Vinylpyridine)/(styrene) comonomers		(4-Vinylpyridine)/(styrene) comonomers	
	Abs(665 cm^{-1})/ Abs(700 cm^{-1}) C–H deformation region	Abs(1226 cm^{-1})/ Abs(1490 cm^{-1}) C–N stretch region	Abs(750 cm^{-1})/ Abs(700 cm^{-1}) C–H deformation region	Abs(1430 cm^{-1})/ Abs(1490 cm^{-1}) C–N stretch region	Abs(820 cm^{-1})/ Abs(700 cm^{-1}) C–H deformation region	Abs(1415 cm^{-1})/ Abs(1490 cm^{-1}) C–N stretch region
A.t.r.-KRS-5-45°	1.10 ± 0.07	0.89 ± 0.10	0.96 ± 0.06	1.37 ± 0.09	0.90 ± 0.07	1.57 ± 0.05
A.t.r.-KRS-5-60°			1.08 ± 0.05	1.39 ± 0.07	1.02 ± 0.09	1.40 ± 0.07
A.t.r.-Ge-60°	1.16 ± 0.08	0.92 ± 0.04	1.21 ± 0.13	1.43 ± 0.04	0.95 ± 0.10	1.40 ± 0.08
T.X.m.	1.23 ± 0.04	0.95 ± 0.10	1.24 ± 0.05	1.49 ± 0.05	1.13 ± 0.03	1.47 ± 0.05

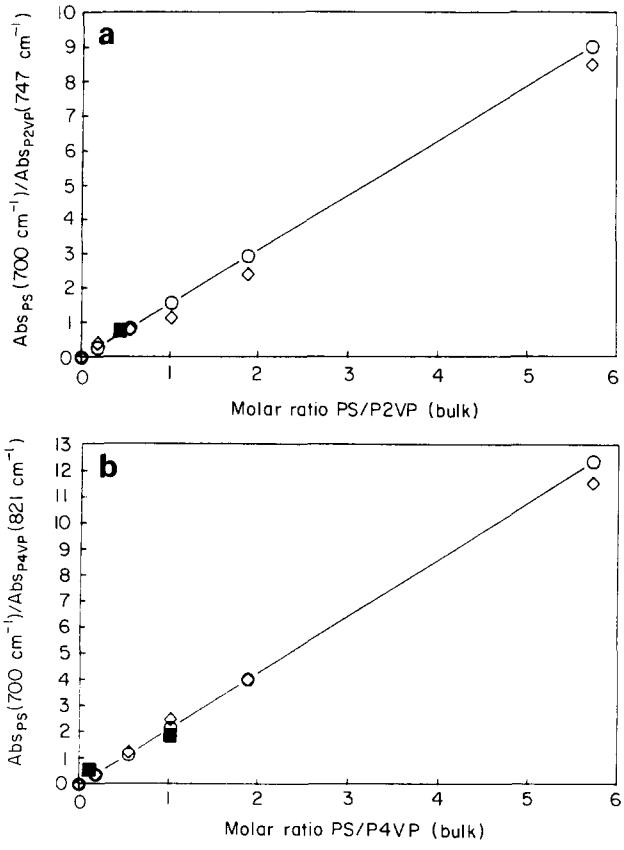

Figure 4 Infra-red Beer's law peak intensity ratio analysis: (a) polystyrene/poly(2-vinylpyridine) (PS/P2VP); (b) polystyrene/poly (4-vinylpyridine) (PS/P4VP). ○, Theoretical values; ◇, blends; ■, copolymers

Table 7 Peak assignments of characteristic positive secondary ions from poly(*N*-vinylpyridine-*co*-styrene) and poly(*N*-vinylimidazole-*co*-styrene)

Secondary fragment ions[a]	m/z
$[C_6H_5]^+$	77
$[C_7H_7]^+$	91
$[C_6NH_7]^+$	92
$[Im + H]^+$	95
$[St + H]^+$	104
$[Py + H]^+$	106
$[Im + Im + H]^+$	187, 189, 191
$[Im + St + H]^+$	197, 199, 201
$[St + St + H]^+$	205, 207, 209
$[Py + St + H]^+$	208, 210, 212
$[Py + Py + H]^+$	209, 211, 213

[a] St, styrene monomer; Im, imidazole monomer; Py, pyridine monomer

polymer surfaces. In particular, the intensity, and therefore the formation probability, of specific ions was directly correlated to the degree of charge stability and availability of specific chemical reactive sites or functionalities located along a given polymer chain[8].

Table 7 lists the possible peak assignments of positive secondary fragment ions from poly(*N*-vinylimidazole-*co*-styrene) and poly(*N*-vinylpyridine-*co*-styrene) copolymers. In addition to the presence of low mass fragment ions (0–150 amu), peaks attributable to the monomer ions of poly(*N*-vinylimidazole) $[Im + H]^+$, polystyrene $[St + H]^+$ and poly(*N*-vinylpyridine) ($N = 2$, 4) $[Py + H]^+$ were detected at $m/z = 95$, 104 and 106, respectively. $[C_6H_6]^+$ peak at $m/z = 77$ has been assigned to the aryl functionality, whereas the $[C_7H_7]^+$

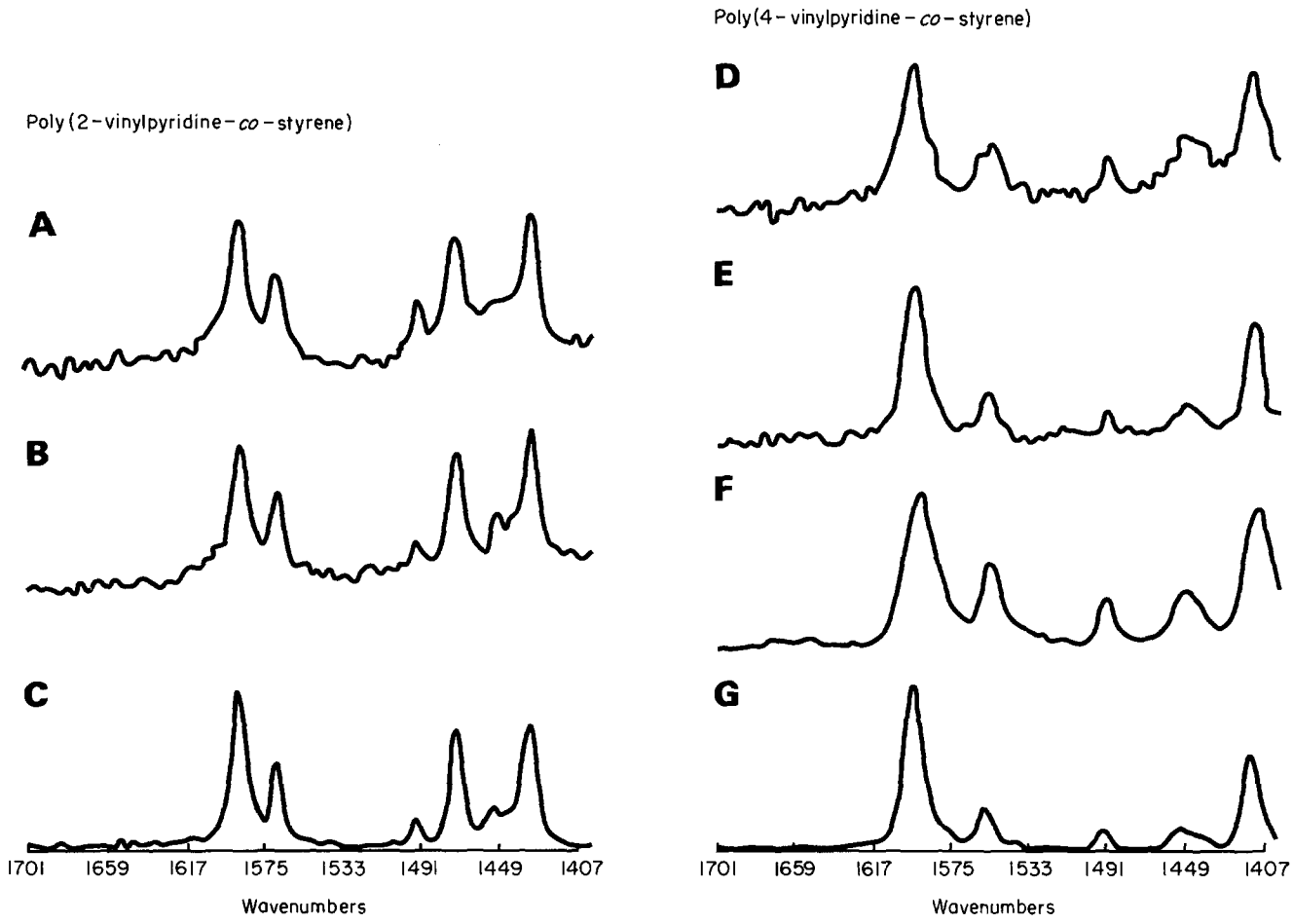

Figure 5 A.t.r. and transmission *FT*i.r. spectra for poly(2-vinylpyridine-*co*-styrene) and poly(4-vinylpyridine-*co*-styrene): A, P2VPS(70/30) 60° Ge a.t.r.; B, P2VPS(70/30) 60° KRS-5 a.t.r.; C, P2VPS(70/30) transmission; D, P4VPS(90/10) 60° Ge a.t.r.; E, P4VPS(90/10) 60° KRS-5 a.t.r.; F, P4VPS(90/10) 45° KRS-5 a.t.r.; G, P4VPS(90/10) transmission

tropylium ion at $m/z = 91$ is characteristic of the styrene component. In the present study, s.i.m.s. analysis of poly(*N*-vinylpyridine-*co*-styrene) samples also shows a sensitivity toward the detection of dimer ions whose ion intensities were related to the statistical sequence distributions in these copolymers. This demonstrated the utility of the s.i.m.s. technique as an analytical tool to determine the sequence of bonding in polymeric matrices. Stabilized dimer ions were also detected and their possible combinations are assigned. Furthermore, acidified samples show an increase in the $[Py + H]^+$ ion distribution (*Figure 6*). In poly(*N*-vinylimidazole-*co*-styrene), the comparison between solution-cast and water-cast films indicated a more significant surface dominance of styrene segments in the water-cast films, represented by a higher $[C_7H_7]^+/[Im + H]^+$ relative ion peak intensity as compared to that in solution-cast films (*Figure 7*). In addition, the technique is quite sensitive to pH differences in the water-cast preparations (*Figure 8*), where a higher $[C_7H_7]^+/[Im + H]^+$ was observed at lower pH due to protonation of the imidazole components.

Electron microscopy

Microphase morphology was not observed in surface and bulk phases of poly(*N*-vinylpyridine-*co*-styrene) samples. In poly(*N*-vinylimidazole-*co*-styrene) water-cast films, styrene microdomains ranging from 200–1000 Å were seen in TEM analysis, comparable to those observed in an earlier study[15] (see *Figure 9*).

DISCUSSION

Earlier ^{13}C n.m.r. analysis of poly(*N*-vinylimidazole-*co*-styrene)[15] and poly(*N*-vinylpyridine-*co*-styrene) in this laboratory established a homogeneous random sequence distribution in both copolymer systems. In addition, poly(*N*-vinylpyridine–styrene) copolymers were examined by d.s.c. analysis, where single glass transition temperatures were observed in these systems. Despite the randomness suggested in terms of bulk structures and compositions, poly(*N*-vinylimidazole-*co*-styrene) displayed microphase separation in the water-cast preparations.

Angle-dependent X.p.s. results from solution-cast films of poly(*N*-vinylimidazole-*co*-styrene) showed an excess of polystyrene in a shallow region (less than about 18 Å) of the air/solid interface. This agrees with our s.i.m.s. data, where a dominance of $[C_7H_7]^+$ ion intensity was detected relative to the imidazole monomer ion intensity. X.p.s. analysis at larger analysis angles (45° and 90°), in conjunction with *FT*i.r.–a.t.r. results indicated a rapid drop-off of polystyrene surface enrichment to bulk values at deeper sampling depths (greater than about 30 Å). In addition, air surface segregation of polystyrene is more pronounced in the water-cast films compared to that in

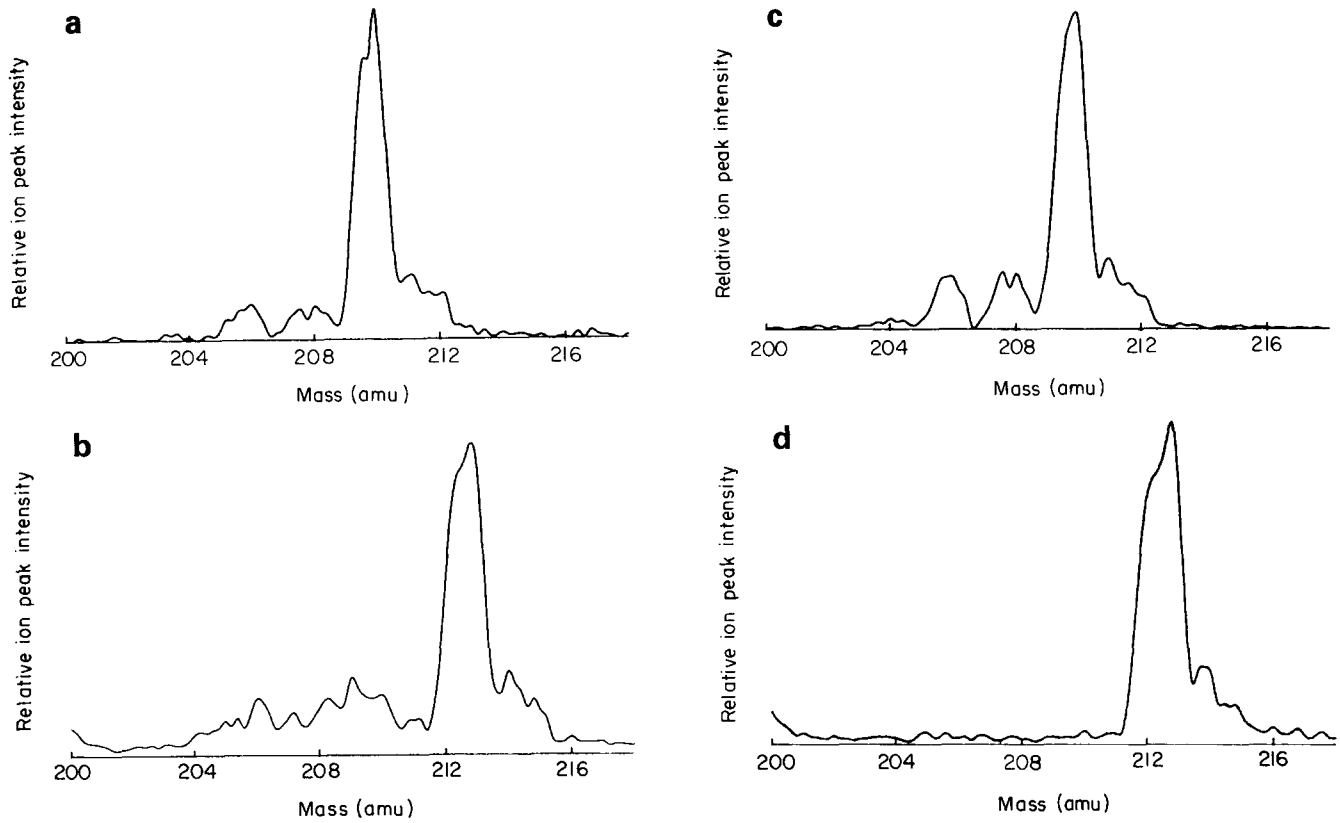

Figure 6 Static s.i.m.s. comparison of dimer regions for solution deposited and acidified films: (a) P2VPS solution deposited on cleaned silver substrate; (b) P2VPS solution deposited on cleaned silver substrate and subsequently reacted with excess amount of HCl; (c) P4VPS solution deposited on cleaned silver substrate; (d) P4VPS solution deposited on cleaned silver and subsequently reacted with excess amount of HCl

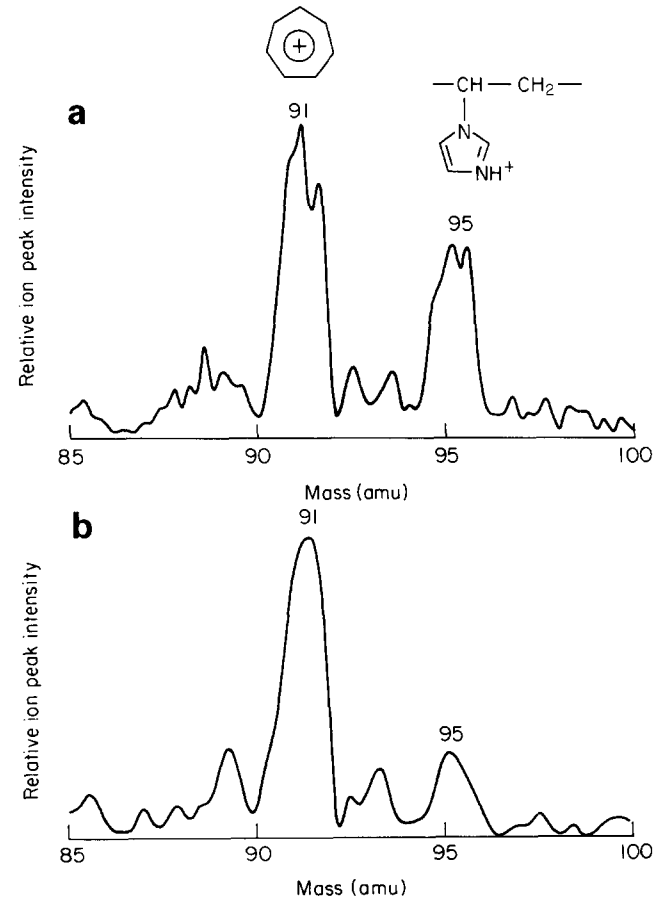

Figure 7 Static s.i.m.s. comparison of solution-cast and water-cast films for poly(*N*-vinylimidazole-*co*-styrene): (a) 20% PVIS solution cast; (b) 2% PVIS water cast

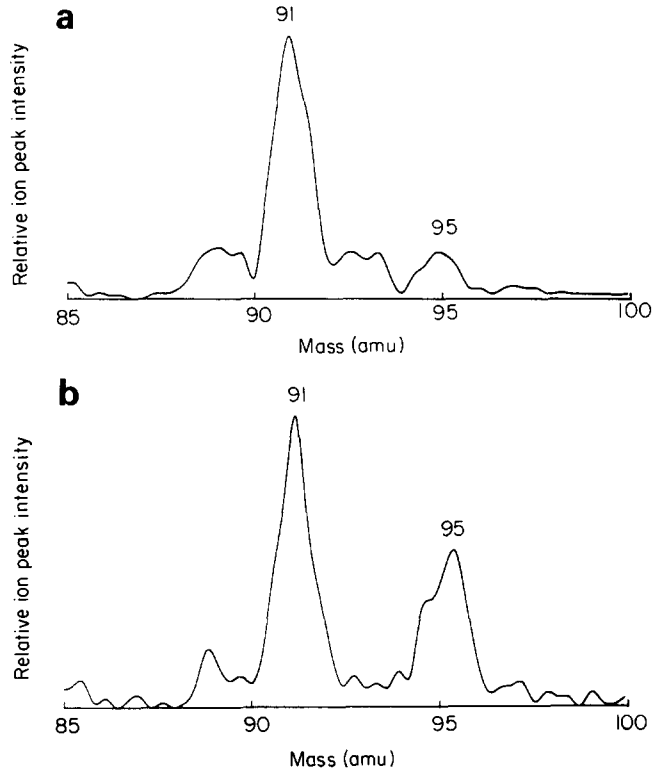

Figure 8 Static s.i.m.s. comparison of poly(*N*-vinylimidazole-*co*-styrene) water-cast films; (a) pH 3.0; (b) pH 9.0

the solution-cast films. On the other hand, poly(*N*-vinylimidazole-*co*-styrene) copolymers are homogeneous over the surface region sampled by each method, and displayed single-phase morphology in EM analysis.

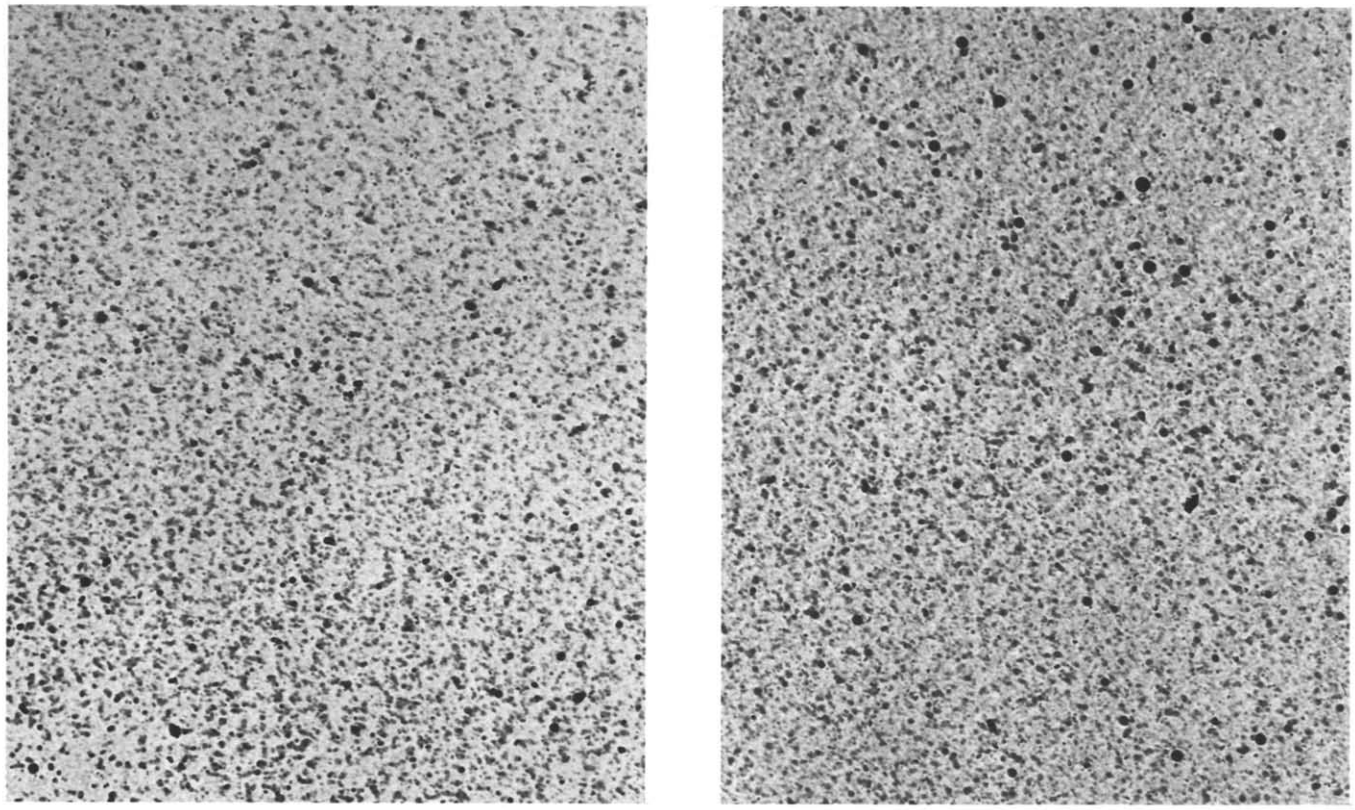

Figure 9 TEM micrographs of poly(*N*-vinylimidazole-*co*-styrene) thin films cast on water from a 2% (w/w) methoxyethanol solution. Scale: 1 mm = 714.3 Å

It is shown in this study that microphase surface segregation can be achieved in selective random copolymer systems through controlled sample preparations. The question as to why microphase separation cannot be induced in the poly(*N*-vinylpyridine-*co*-styrene) ($N = 2, 4$) may be attributed to the differences in hydrophobicities among the copolymer systems. In order to obtain phase separation in aqueous media, one must recognize the compensating effects of electrostatic repulsions between the protonated species and the hydrophobic attractions among the styrene groups. The pyridine moiety is a weaker base and less hydrophilic than the corresponding imidazole functionality, hence the competition between the attractive hydrophobic interactions among styrene segments and the repulsive electrostatic interactions among protonated pyridine groups is not significant enough to induce phase separation in the poly(*N*-vinylpyridine-*co*-styrene) systems. On the other hand, due to a higher basicity of imidazole component, we would expect a stronger affinity of the imidazole segments to water molecules via formation of hydrogen bonds occurring between water molecules and the unshared electron pair of the N atom in the imidazole moiety. Correspondingly, the extent of hydrogen bonding in the poly(*N*-vinylpyridine-*co*-styrene) is presumably occurring to a lesser degree.

In an attempt to compare the extent of surface hydrophobicity/hydrophilicity between poly(*N*-vinylimidazole-*co*-styrene) and poly(*N*-vinylpyridine-*co*-styrene) in aqueous media as a function of pH, contact angle measurements were performed to complement our spectroscopic and microscopic data. This approach is adopted based on a previous study[23], in which contact angle measurements were used to monitor the extent of ionization of near-surface carboxylic acid groups on low-density polyethylene films. *Figure 10* shows the plot of advancing contact angle measured as a function of pH. In the wettability behaviour of poly(*N*-vinylimidazole-*co*-styrene), higher advancing contact angles were observed at all regions above pH 1.5, which is indicative of the more hydrophobic character in its near-surface region (about 5 Å). In addition, a lower apparent pKa is evident in this system, which is expected based on its higher basicity. The contact angle measurements agree well with the previously discussed X.p.s. and s.i.m.s. data, where surface excess of polystyrene is suggested in this random copolymer system.

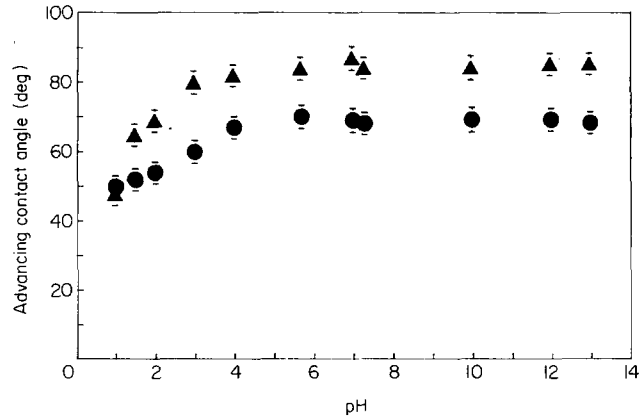

Figure 10 Advancing contact angle *versus* pH: ▲, poly(*N*-vinylimidazole-*co*-styrene); ●, poly(*N*-vinylpyridine-*co*-styrene)

CONCLUSIONS

In this study, a combination of analytical spectroscopic and microscopic techniques was employed to characterize the surface of a series of nitrogen-containing random copolymers. Their overall surface microstructural, compositional and morphological profiles were examined under selective sample preparations. Angle-dependent X.p.s. and s.i.m.s. results from poly(*N*-vinylimidazole-*co*-styrene) imply a preferential segregation of polystyrene to a region less than 30 Å from the air/solid interface. Analysis at deeper regions (take-off angles of 45° and 90°) and *FT*i.r.–a.t.r. results show a rapid drop-off to bulk values. The application of multitechnique investigation of poly(*N*-vinylimidazole-*co*-styrene) ($N = 2, 4$) systems yields equivalent surface and bulk compositions and functionalities under an identical set of experimental controls. It is also shown that s.i.m.s. analysis of polymeric materials can differentiate structural and bonding variations, attributable to its unique sensitivity toward detection of *n*-mer ions.

ACKNOWLEDGEMENTS

This investigation was supported by the National Science Foundation, Division of Materials Research Polymer Program, under grant no. 8720650. We thank Dr Julia S. Tan of Eastman Kodak Company for her generous donation of the poly(*N*-vinylimidazole)–polystyrene copolymer, Dr Philip Kumler from SUNY at Fredonia for the d.s.c. measurements and Dr Robert Osteryoung from SUNY at Buffalo for the use of the *FT*i.r. spectrometer.

REFERENCES

1 Platzer, N. in 'Applied Polymer Science' (Eds R. W. Tess and G. W. Poehlein), ACS Symposium Series 285, American Chemical Society, Washington, DC, 1985, p. 220
2 Odian, G. 'Principles of Polymerization', John Wiley & Sons, New York, 1981, p. 495
3 Noshay, A. and McGrath, J. E. 'Block Copolymers:Overview and Critical Survey', Academic Press, New York, 1977, p. 30
4 Rosen, S. L. 'Fundamental Principles of Polymeric Materials', John Wiley & Sons, New York, 1982, p. 14
5 Noshay, A. and McGrath, J. E. 'Block Copolymers: Overview and Critical Survey', Academic Press, New York, 1977, p. 10
6 Clark, M. B. Jr, Burkhardt, C. A. and Gardella, J. A. Jr *Macromolecules* 1989, **22**, 4495
7 Schmidt, J. J., Gardella, J. A. Jr and Salvati, L. Jr *Macromolecules* 1989, **22**, 4489
8 Hook, K. J., Hook, T. J., Wandass, J. H. and Gardella, J. A. Jr *Appl. Surf. Sci.* 1990, **44**, 29
9 Schmitt, R. L., Gardella, J. A. Jr, Magill, J. H., Chin, R. L. and Salvati, L. Jr *Polymer* 1987, **28**, 1462
10 Hook, K. J. and Gardella, J. A. Jr *J. Vac. Sci. Technol.* 1987, **A5**(4), 1332
11 Schmitt, R. L., Gardella, J. A. Jr and Salvati, L. Jr *Macromolecules* 1986, **19**(3), 648
12 Ishizu, K., Hayashi, T. and Fukutomi, T. *Makromol. Chem.* 1987, **189**, 753
13 Ishizu, K. *Polymer* 1989, **30**, 793
14 Moller, M. and Lenz, R. W. *Makromol. Chem.* 1989, **190**, 1153
15 Sutton, R. C., Thai, L., Hewitt, J. M., Voycheck, C. L. and Tan, J. S. *Macromolecules* 1988, **21**, 2432
16 Eng, F. P. and Ishida, H. *J. Electrochem. Soc.* 1988, **135**(3), 603
17 Seah, M. P. in 'Practical Surface Analysis by Auger and X-ray Photoelectron Spectroscopy' (Eds D. Briggs and M. P. Seah), John Wiley & Sons, New York, 1983, p. 208
18 Wandass, J. H., Schmitt, R. L. and Gardella, J. A. Jr *Appl. Surf. Sci.* 1989, **40**, 85
19 Vargo, T. G. and Gardella, J. A. Jr *J. Vac. Sci. Tech. A* 1989, **7**, 1733
20 Seah, M. P. and Dench, W. A. *Surf. Interf. Anal.* 1979, **1**(1), 2
21 Briggs, D. in 'Handbook of X-Ray and Ultraviolet Photoelectron Spectroscopy' (Ed. D. Briggs), Heyden and Son, London, 1977, p. 153
22 Mittlefehldt, E. R. and Gardella, J. A. Jr *Appl. Spectrosc.* 1989, **43**(7), 1172
23 Holmes-Farley, S. R., Reamey, R. H., McCarthy, T. J., Deutch, J. and Whitesides, G. M. *Langmuir* 1985, **1**, 725
24 Clark, M. B. Jr, Gardella, J. A. Jr, Schultz, T. M., Patil, D. G. and Salvati, L. Jr *Anal. Chem.* 1990, **62**, 949